INTERNATIONAL JOURNAL OF MICROWAVE AND OPTICAL TECHNOLOGY,
VOL.9, NO.4, JULY 2014

Investigation of a New Radiating Mode in Rectangular Dielectric Resonator Antenna: Experimental Validation

G. D. Makwana, Deepak Ghodgaonkar, Sanjeev Gupta

Dhirubhai Ambani Institute of Information and Communication Technology (DA-IICT)
Near Indroda Circle, Gandhinagar – 382007, Gujarat, India.
E-mail: gmakwana@gmail.com, deepak_ghodgaonkar@daiict.ac.in, sanjeev_gupta@daiict.ac.in

***Abstract*-In the past, a $TE^x_{\delta 01}$ mode had been proposed with two metal strips on the side walls of a rectangular dielectric resonator antenna (RDRA) as well as hybrid rectangular dielectric-air-metal strips composite resonator antenna. In this paper, a new radiating $TE^x_{\delta 10}$ mode in the RDRA is proposed by placing single metal strip on top surface. To validate the $TE^x_{\delta 10}$ mode and a conventional lowest order $TE^x_{\delta 11}$ mode, simple RDRA with and without a metal strip is designed, fabricated, and measured. The RDRA is mounted on the grounded substrate and fed by a simple microstrip line. Based on parametric study and electric field distributions, dimension along the y-axis is principally used to determine the resonant frequency of the proposed mode. The proposed mode has an impedance bandwidth of 35 MHz at 2.24 GHz and gain of 2.35 dBi. The radiating $TE^x_{\delta 10}$ mode has broadside radiation patterns. As compared to the conventional $TE^x_{\delta 11}$ mode, reduction in the resonant frequency and the impedance bandwidth by 58% and 79% is observed in the new mode.**

***Index Terms*- Rectangular dielectric resonator antenna, conventional mode, new radiating mode.**

I. INTRODUCTION

The dielectric resonator antennas (DRAs), introduced by Long et al. in 1983 [1], could be used in numerous wireless communication and sensing applications due to many advantageous features they possess. These include high radiation efficiency, compact size, light weight, and the versatility in the shapes, and feeding mechanism. There are three basic shapes available for common design, including rectangular, cylindrical, and spherical. Among these, the rectangular DRAs (RDRAs) show some advantages over other shapes. Such as, three available dimensions provide two degree of freedom (one more than the cylindrical one and two more than the spherical one), making it most flexible in designs. In practice, the rectangular DRAs are much easier to fabricate. Also, mode degeneracy can be avoided by properly choosing the dimensions. Hence it is preferred in DRA design [2].

Different modes with different antenna characteristics and radiation patterns are possible in the RDRA. TE modes are typically excited, which can be divided into TE^x, TE^y, and TE^z modes, in the RDRA mounted on a ground plane. Depending on the relationship of the three dimensions and way of exciting mechanism, a conventional dominant mode is one of $TE^x_{\delta 11}$, $TE^y_{1\delta 1}$, and $TE^z_{11\delta}$ $(0 < \delta < 1)$. The mode subscripts refer to field variation along the x-, y-, and z-axis respectively. Higher-order modes can also be excited for certain aspect ratios, such as $TE^x_{\delta n1}$, $TE^x_{\delta 1n}$ modes (n = 2, 3...) as shown in Figure 1. However, not all higher modes have similar broadside patterns as shown by the basic mode. A $TE^x_{\delta 21}$ mode shown in Figure 1 has a null at broadside. Resonant frequency of these modes is a function of the three dimensions and dielectric constant, according to dielectric waveguide model (DWM) [3].

Recently, new radiating $TE^x_{\delta 01}$ mode reported in [4] with two metal strips placed on side walls, perpendicular to the ground plane in hybrid RDRA mounted on the ground plane and fed by a

INTERNATIONAL JOURNAL OF MICROWAVE AND OPTICAL TECHNOLOGY,
VOL.9, NO.4, JULY 2014

coupling slot. This mode can work at a much lower frequency than the conventional mode in

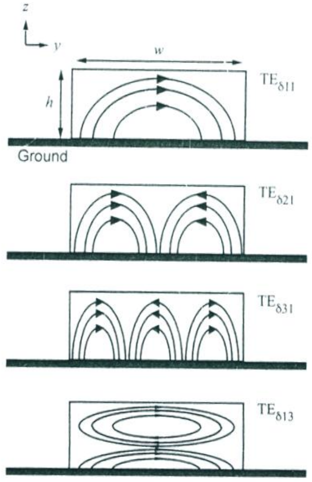

Fig.1 Field distributions of the modes in RDRA [3]

the RDRA with the same dimensions. Also, $TE^{x}_{\delta 01}$ mode [5] demonstrated in hybrid rectangular dielectric-air-metal strips composite resonator antenna. The mode had been excited using two shorting metal strips connected at two ends of the RDRA, one metal strip with a rectangular shape, the other with a T-shape. The feeding mechanism adopted another T-shaped metal strip attached to the bottom face of the DR and connected to the inner conductor of the coaxial probe.

In this paper, a rectangular DRA with and without single metal strip placed on top surface is described. The new $TE^{x}_{\delta 10}$ radiating mode is proposed and compared to the conventional dominant mode, $TE^{x}_{\delta 11}$. Parametric study has been carried out on the proposed mode. Specific field distributions of the new mode and the conventional mode are discussed. Measured return loss, radiation patterns, bandwidth, and gain are compared with simulated results of the $TE^{x}_{\delta 10}$ mode and show high agreement.

II. ANTENNA CONFIGURATION

Geometry of the conventional and proposed rectangular dielectric resonator antenna (RDRA) is shown in Figure 2 (a) and (b) respectively. The geometry without metal patch/strip is for the conventional $TE^{x}_{\delta 11}$ mode, while the geometry with metal strip on top surface of RDRA is for proposed new $TE^{x}_{\delta 10}$ mode. A 50 Ω microstrip line is printed on a grounded substrate. The grounded substrate has dimension of W_1 x L_1 x H_1 with dielectric constant, ε_s = 2.5. The rectangular DRA is placed on open ended microstrip line for efficient coupling. The rectangular DRA has a depth d, a width w, and height h along x-, y- and z-axis respectively. The ceramic material with relative dielectric constant ε_r = 32 is used to fabricate the DR. A metal strip (d x w) is placed on the top surface of the RDRA in the xy-plane. The metal strip could be roughly modeled an infinitely thin perfect electric conductor (PEC). Apart from the conventional RDRA, the proposed DRA has two surfaces which are roughly PEC and remaining four surfaces are roughly perfect magnetic conductor (PMC). An interface between high dielectric and air is PMC.

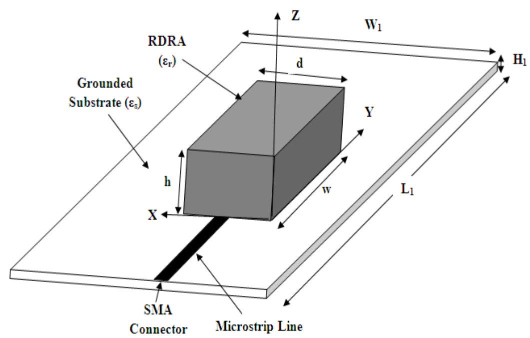

(a)

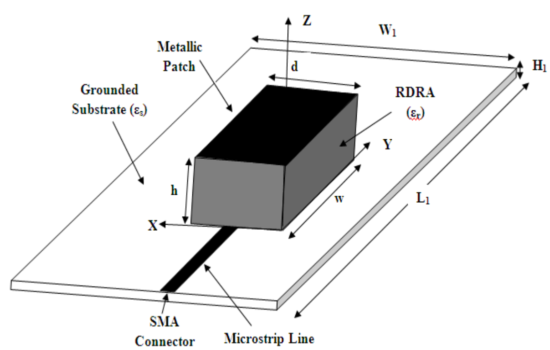

(b)

Fig.2 Geometry of (a) the conventional RDRA [2], (b) the proposed RDRA

INTERNATIONAL JOURNAL OF MICROWAVE AND OPTICAL TECHNOLOGY,
VOL.9, NO.4, JULY 2014

III. NUMERICAL STUDY

Commercial 3-D full-wave electromagnetic simulation software Ansoft HFSS, based on finite element method, is used for the numerical study. RDRA with w = 17 mm, d = 7 mm, h = 3 mm is simulated with the proposed geometry as well as the conventional geometry and is resonated at 2.19 GHz and 5.38 GHz respectively. Simulated electric field distributions at resonance in the proposed antenna and the conventional antenna are shown in Figure 3. Arrow indicates the direction of the field. Color represents strength of the field. For the conventional $TE^x_{\delta 11}$ mode, the E-field patterns are sketch in Figure 3 (a), (b), (c) while for the new $TE^x_{\delta 10}$ mode; the E-field patterns are sketch in Figure 3 (e), (f), (g) for xy, zx and yz -plane respectively.

For the conventional $TE^x_{\delta 11}$ mode, from the Figure 3(c), the E-fields circulate around the x-axis and vary in both, along the y-axis and the

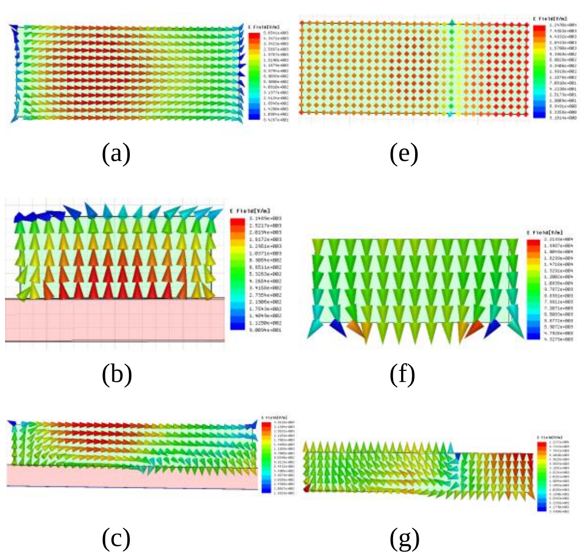

Fig. 3 Simulated E-vector field at 5.38 GHz for the conventional $TE^x_{\delta 11}$ mode (a) xy- plane, (b) zx- plane, (c) yz-plane, at 2.19 GHz for the new mode $TE^x_{\delta 10}$ mode (e) xy- plane, (f) zx- plane, (g) yz- plane

z-axis. Thus, E_y and E_z are predominant whereas, E_x is uniformly distributed along x-axis. These distributions are due to boundary conditions of the DR in zx-plane. Interface between the microwave material and air in the zx-plane can be seen an imperfect magnetic wall, which could support E-field parallel to the interface and H-field perpendicular to the interface. From the Figure 3(b), the E-field is oriented in the z-axis and varies from maximum to zero as the height increases from the ground plane to the top surface of the DR. E-fields along the x-axis are uniformly distributed and small variation, $\delta < 1$ along the x-axis. From the Figure 3(a), E-fields along x-axis are uniformly distributed. The electric field is oriented along the y-axis and variation in this direction shown in Figure 3(a).

For the proposed $TE^x_{\delta 10}$ mode, from Figure 3(g), the E-fields circulate around the x-axis and change in along the y-axis and z-axis. This similarity is due to the same boundary condition as the conventional one in zx-plane. From the Figure 3(f), E-fields are oriented along the z-axis and homogenously distributed in the same direction. There are no field variations from the ground plane to the top surface of the antenna along z-axis. Also, E-fields along the x-axis are minor δ variation. As compared to the conventional mode, different field distributions in the zx-plane are due to different boundary conditions in the xy-plane. From the Figure 3(e), electric fields are along z-axis and uniformly distributed along x- and y-axis. This change of distributions as compared to the $TE^x_{\delta 11}$ mode is due to the metal strip on the top surface of the RDRA in the xy-plane. The metal strip can be modeled as an electric wall, which supports E-field component perpendicular to the surface and H-field component parallel to the interface. Fig 4 sketches the H-fields in the both antennas at resonance. The H_x component is dominant along center of the RDRA for both modes.

The resonant frequency of the $TE^x_{\delta 10}$ mode can be derived by the DWM and mixed magnetic wall (MMW) model in [2]. As compared to the conventional RDRA mounted on the ground plane, the proposed antenna has different boundary conditions. The PMC boundary condition $E \cdot n = 0$ is assumed at y = 0 and y = w.

INTERNATIONAL JOURNAL OF MICROWAVE AND OPTICAL TECHNOLOGY,
VOL.9, NO.4, JULY 2014

The imperfect PMC boundary condition is assumed at x = 0 and x = d. The PEC boundary condition at z = h. Because of two horizontal metal strips (one at bottom of the substrate and other at z = h) in the xy-plane, wave number along the z-direction is reduced to zero. Following equations are obtained for k_y and k_z:

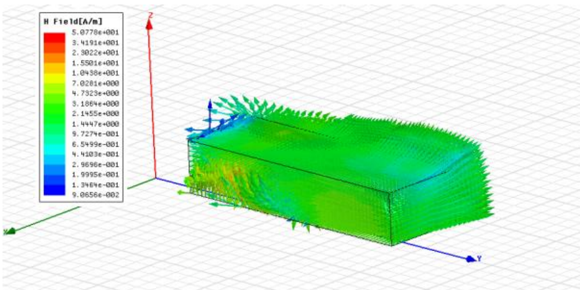

(a)

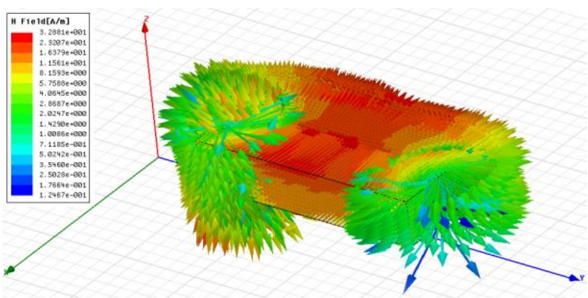

(b)

Fig.4 Simulated H-vector field (a) at 5.38 GHz for the conventional $TE^x_{\delta 11}$ mode, (b) at 2.19 GHz for the new mode $TE^x_{\delta 10}$ mode

$$k_y = \frac{\pi}{w},\ k_z = 0,\ k_o = \frac{2\pi}{\lambda_0} \qquad (1)$$

Where, k_0 denotes free-space wave number corresponding to resonant frequency. The wave numbers also satisfy the following separation equation:

$$k_x^2 + k_y^2 = k_0^2 \qquad (2)$$

The resonant frequency of the $TE^x_{\delta 10}$ mode is found by solving a following transcendental equation:

$$k_x \tan\left(k_x \frac{d}{2}\right) = \sqrt{(\varepsilon_r - 1)k_0^2 - k_x^2} \qquad (3)$$

For given resonant frequency of the new mode, RDRA parameters such as ε_r, w, and d, the wave number k_x determined using (1) and (2) and also satisfies (3). By using DWM and MMW model, the following field components within the RDRA for the new mode are:

$$H_x = \frac{k_y^2}{j\omega\mu_0}\cos(k_x x)\cos(k_y y) \qquad (4)$$

$$H_y = \frac{k_y k_x}{j\omega\mu_0}\sin(k_x x)\sin(k_y y) \qquad (5)$$

$$E_z = -k_y \cos(k_x x)\sin(k_y y) \qquad (6)$$

$$E_x = E_y = H_z = 0 \qquad (7)$$

H_x component is dominant along the center of the RDRA, while the E-fields (predominantly E_z) circulate around the H_x component. From the field distributions and theoretical analysis, the new mode is achievable in the RDRA. Calculated resonant frequency is 5.34 GHz (0.73% of error) for the conventional mode, while 2.33 GHz for the new mode (5.93% of error).

IV. PARAMERIC STUDIES

To validate the new radiating mode, parametric study has been performed on different dimensions of the proposed RDRA. The study is carried out by varying one dimension, while others are invariable. The purpose of study is to see effect on resonant frequency of $TE^x_{\delta 10}$ mode. Return loss characteristics of the proposed mode due to the variation of width w, depth d, and height h of RDRA are shown in Fig. 5(a), (b), and (c) respectively. From Fig. 5(a), it is observed that when dimension along the y-axis (w) is increased from 13 mm to 21 mm, the resonant frequency is decreased from 2.61 GHz

INTERNATIONAL JOURNAL OF MICROWAVE AND OPTICAL TECHNOLOGY,
VOL.9, NO.4, JULY 2014

to 1.75 GHz. It is found that when dimension along the x-axis (d) is increased from 5 mm to 9 mm, the resonant frequency of the $TE^{x}_{\delta 10}$ mode is very minor variation from 2.23 GHz to 2.07 GHz as shown in Fig. 5(b). From the Fig. 5(c), it is noticed that the resonant frequency of the mode almost remain stable when dimension along the z-axis (h) is increased from 2 mm to 5 mm.

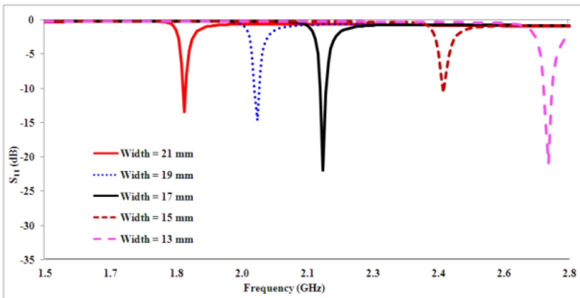

(a)

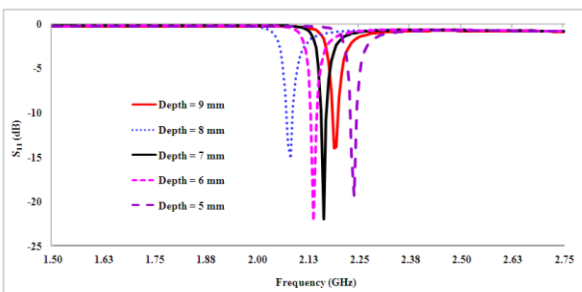

(b)

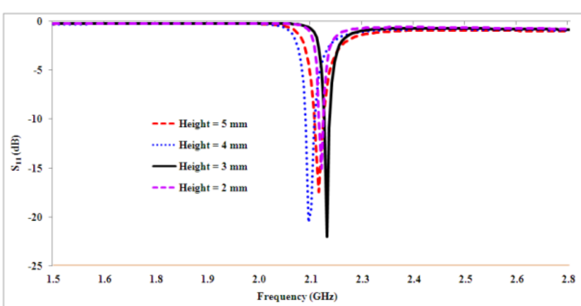

(c)

Fig. 5 Simulated S_{11} of the proposed antenna with different value of (a) length w (d = 7 mm, h = 3 mm), (b) depth d (w = 17 mm, h = 3 mm), (c) Height h (w = 17 mm, d = 7 mm)

From these characteristics, it is observed that the resonant frequency of the new mode is mainly depends on width w, and slightly depend on depth d. Thus, the degree of freedom for the proposed antenna design is one as compared to two degree of freedom in the conventional RDRA design. This is also confirmed by specific field distributions as given in Figure 3 and 4.This observation is also verify by equations (1-3) for determination of resonant frequency of the $TE^{x}_{\delta 10}$ mode.

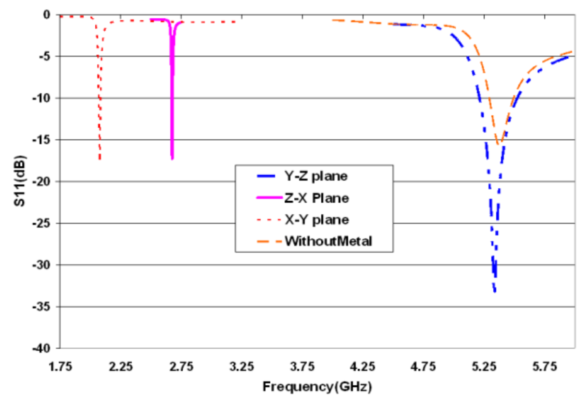

Fig. 6 Simulated S_{11} for metal strip placed at different surfaces of the RDRA

The simulation is also carried out for a metal strip placed at different side walls of the RDRA. A metal strip is placed at z = h (xy-plane), x = d (yz-plane), y = w (zx-plane), and without metal strip: these four cases are simulated and return loss characteristics are shown in Fig. 6. Resonant frequency (calculated & simulated), impedance bandwidth etc are listed in Table 1. It is observed that the resonant frequency and impedance bandwidth are drastically decreased due to the metal strip at xy-plane and zx-plane as compared to the without metal strip on RDRA, while resonant frequency is nearly same for the metal strip at yz-plane with increase of bandwidth as compared to the conventional RDRA. From these, it is noticed that by placing a metal strip at appropriate surface, the new radiating mode is possible to excite in the rectangular DRA.

IJMOT

INTERNATIONAL JOURNAL OF MICROWAVE AND OPTICAL TECHNOLOGY,
VOL.9, NO.4, JULY 2014

Table 1 Effect of a metal strip on surfaces of RDRA

Position of Metal Strip	Calc. Fr., GHz	Sim. Fr., GHz	% of Error	BW, MHz	% of BW
xy plane (z=h)	2.33	2.19	6.00	35	1.20
zx-plane(y=w)	2.45	2.68	8.36	10	0.37
yz-plane(x= d)	5.07	5.33	5.17	310	5.81
Without strip	5.37	5.38	0.92	210	3.89

V. EXPERIMENTAL RESULTS

For further confirmation of the new radiating $TE^{x}_{\delta 10}$ mode, based on extensive simulation, the proposed RDRA design and the conventional RDRA design are fabricated and measured. The physical parameters of both the antennas are d = 7 mm, w = 17 mm, h = 3 mm, $\varepsilon_r = 32$. The return loss characteristics of these prototypes are measured by an Agilent vector network analyzer. Figure 7 (a), and (b) show the measured and simulated return loss characteristics of the proposed designs and the conventional designs respectively.

Measured parameters such as resonant frequency, impedance bandwidth, % of bandwidth, boresight gain, HPBW and simulated radiation efficiency are listed in Table 2 for the $TE^{x}_{\delta 10}$ and $TE^{x}_{\delta 11}$ mode. From Figure 7 (a), Table 2, it is noticed that proposed antenna is resonated at 2.24 GHz for $TE^{x}_{\delta 10}$ mode with a bandwidth of 35 MHz, covering frequency band of 2.223-2.258 GHz, which are agree with the simulated results. At resonant, measured gain is 2.35 dBi. The conventional $TE^{x}_{\delta 11}$ mode is resonated at 5.39 GHz and having bandwidth of 165 MHz. With reference to the conventional mode, resonant frequency and bandwidth of the $TE^{x}_{\delta 10}$ mode are decreased by 58% and 79% respectively.

From these results, it is concluded that by a metal strip on the top surface of the RDRA, the new mode is excited whose frequency is much smaller than the conventional mode. Also the bandwidth of the proposed mode is narrower than that of the conventional one.

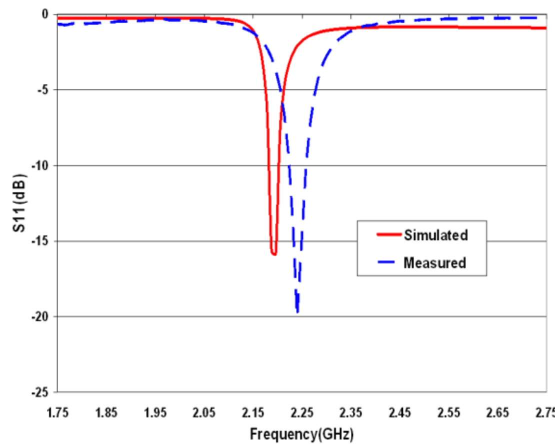

(a)

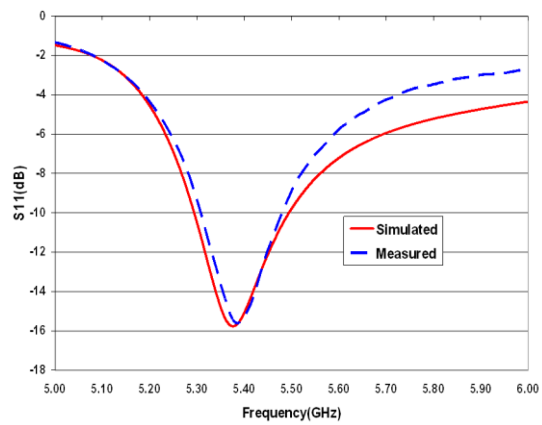

(b)

Fig. 7 Measured and simulated return loss characteristics of (a) the proposed $TE^{x}_{\delta 10\ mode}$, and (b) the conventional $TE^{x}_{\delta 11}$ mode

Table 2 Measured parameters of the proposed and conventional mode

Parameters	$TE^{x}_{\delta 10}$	$TE^{x}_{\delta 11}$
Resonant Frequency (GHz)	2.24	5.39
Bandwidth (MHz)	35	165
% of Bandwidth	1.56	3.56
Gain at bore site (dBi)	2.35	1.62
HPBW	90°	92°
Simu, radiation efficiency	94.79%	98.41%
Reduction in Freq.	58.44 %	---
Reduction in BW	78.78 %	----

Field radiation patterns at resonant are measured in anechoic chamber for the proposed mode. For proposed mode, measured and simulated E-plane radiation patterns are shown in Fig. 8 (a), while

INTERNATIONAL JOURNAL OF MICROWAVE AND OPTICAL TECHNOLOGY,
VOL.9, NO.4, JULY 2014

measured and simulated H-plane patterns are sketched in Fig. 8 (b). It is seen that the $TE^{x}_{\delta 10}$ mode has broadside radiation patterns in both principal planes. Measured cross-polar rejection is better than 20 dB in the E-plane, while it is better than 15 dB in the H-plane. The measured patterns are well accordance with the simulated patterns. Fig 9 shows measured and simulated gain of the proposed mode. Simulated radiation efficiency for the $TE^{x}_{\delta 10}$ mode is around 94.79% while for the $TE^{x}_{\delta 11}$ mode; it is around 98.41%.

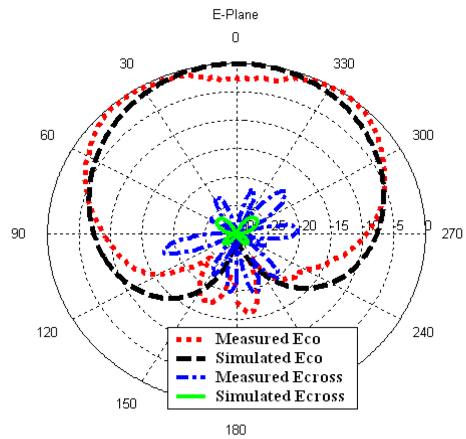

(a)

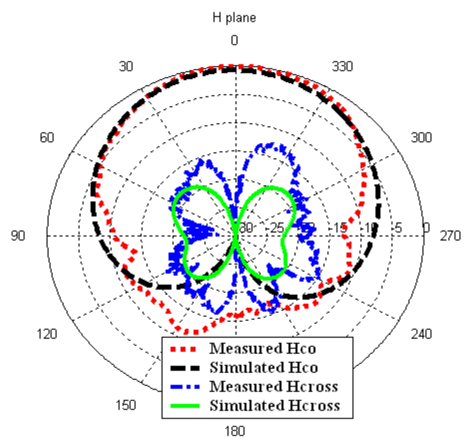

(b)

Fig. 8 Measured and simulated radiation patterns for the proposed mode at resonant (a) E-plane and (b) H-plane for the proposed mode

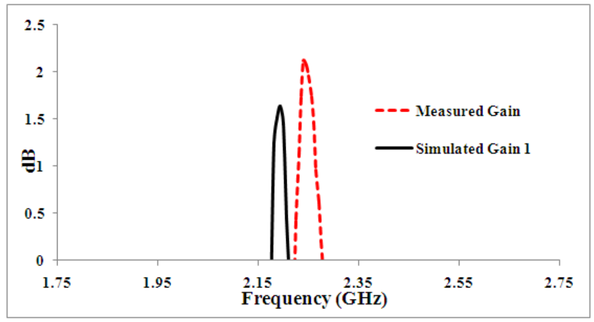

Fig. 9 Measured and simulated gain for the proposed mode

The reduction of efficiency in the proposed mode is due to the conductor losses in additional metal strip as compared to the conventional RDRA. The measured results of the proposed new $TE^{x}_{\delta 10}$ mode are compared with the published results of a $TE^{x}_{\delta 01}$ mode in Table 3 for validation. From the Table 3, it is observed that proposed method of the new radiating mode is easy to fabricate due to simple structure and feeding mechanism.

Table 3 Comparison of the results of the $TE^{x}_{\delta 10}$ mode with other published new $TE^{x}_{\delta 01}$ mode

Particulars	$TE^{x}_{\delta 01}$ [4]	$TE^{x}_{\delta 01}$ [5]	Proposed $TE^{x}_{\delta 10}$
DR dimensions w x d x h mm^3	15x15x16	25x6x3.9	17x7x3
ε_r	10	90	32
Fr (GHz) Theory	2.091	---	2.330
Fr (GHz) Exp	1.741	3.500	2.240
Freq. Range (GHz)	1.716-1.767	3.465-3.550	2.223-2.258
BW (MHz)	51	85	35
Feeding	Slot Coupled	T-Shaped Strip with coaxial cable	Microstrip Line
Structure	RDRA + 2 metal strips	RDRA + air gap + 2 metal strips	RDRA + a metal strip

VI. CONCLUSION

In this paper, a new radiating $TE^{x}_{\delta 10}$ mode is proposed by using a metal strip placed on top surface of the RDRA. From simulated field distributions, it is confirmed that the new mode has been excited in the proposed RDRA design. Theoretical analysis is also supported the

INTERNATIONAL JOURNAL OF MICROWAVE AND OPTICAL TECHNOLOGY,
VOL.9, NO.4, JULY 2014

proposed mode in the RDRA. By parametric study, resonant frequency of the $TE^x_{\delta 10}$ mode is mainly determined by width, little affected by depth, and stable with change in height. The proposed design is fabricated, measured and compared with the $TE^x_{\delta 11}$ mode. For the $TE^x_{\delta 10}$ mode, all critical measured results are compared with the simulated results and show high agreement. From the measured results, the new mode is confirmed. It is observed that the $TE^x_{\delta 10}$ mode work at lower frequency than the $TE^x_{\delta 11}$ mode in the RDRA with the same dimensions. The $TE^x_{\delta 10}$ mode has a broadside radiation patterns as the conventional mode has. Compared to $TE^x_{\delta 11}$ mode, the proposed mode can be excited in a more compact structure, and lower impedance bandwidth, if both mode work at same frequency.

ACKNOWLEDGMENT

We would like to thank Prof. K. J. Vinoy, Microwave Laboratory, Indian Institute of Science, Bangalore, India for his continuous support and guidance to carry out measurements.

REFERENCES

[1] S.A. Long, M.W. McAllister, and L.C. Shen, "Rectangular dielectric resonator antenna," *IEEE Electronics Letters*, Vol. 19, pp. 218-219,1983.

[2] A. Ittipiboon, R. K. Mongia, "`Theoretical and experimental investigation on rectangular dielectric resonator antennas", *IEEE Transactions on Antennas & Propagation*, Vol. 45, No. 9, pp. 1348-1356,1997.

[3] A. Petosa, Dielectric Resonator Antenna Handbook, Artech House, 2007.

[4] Y. Gao, Z. Feng, and L. Zhang, "Investigation of a new radiating mode and the traditional dominant mode in rectangular dielectric resonator antenna", *IEEE Antennas and Wireless Propagation Letters*, Vol. 11, pp.909--912, 2012.

[5] Y. Gao , Z. Feng, and L. Zhang, "Experimental investigation of new radiating mode in rectangular hybrid dielectric resonator antenna", *IEEE Antennas and Wireless Propagation Letters*, Vol. 10, pp.91-94, 2011.